Electroactive Spinal Instrumentation for Targeted Osteogenesis and Spine Fusion: A Computational Study

Saad Javeed, Justin K. Zhang, Jacob K. Greenberg, Christopher F. Dibble, Eric Zellmer, Dan Moran, Eric C. Leuthardt, Wilson Z. Ray and Matthew R. MacEwan

This information is current as of May 17, 2025.

Email Alerts	Receive free email-alerts when new articles cite this article. Sign up at:
	http://ijssurgery.com/alerts

Electroactive Spinal Instrumentation for Targeted Osteogenesis and Spine Fusion: A Computational Study

SAAD JAVEED, MBBS[1]; JUSTIN K. ZHANG, BS[1]; JACOB K. GREENBERG, MD, MSCI[1]; CHRISTOPHER F. DIBBLE, MD, PhD[1]; ERIC ZELLMER, PhD[2]; DAN MORAN, PhD[2]; ERIC C. LEUTHARDT, MD[1,2]; WILSON Z. RAY, MD[1,2]; AND MATTHEW R. MACEWAN, PhD[1,2]

[1]*Department of Neurosurgery, Washington University School of Medicine, St. Louis, MO, USA;* [2]*Department of Biomedical Engineering, Washington University School of Medicine, St. Louis, MO, USA*

ABSTRACT

Background: Direct current electrical stimulation may serve as a promising nonpharmacological adjunct promoting osteogenesis and fusion. The aim of this study was to evaluate the utility of electroactive spine instrumentation in the focal delivery of therapeutic electrical stimulation to enhance lumbar bone formation and interbody fusion.

Methods: A finite element model of adult human lumbar spine (L4-L5) instrumented with single-level electroactive pedicle screws was simulated. Direct current electrical stimulation was routed through anodized electroactive pedicle screws to target regions of fusion. The electrical fields generated by electroactive pedicle screws were evaluated in various tissue compartments including isotropic tissue volumes, cortical, and trabecular bone. Electrical field distributions at various stimulation amplitudes (20–100 μA) and pedicle screw anodization patterns were analyzed in target regions of fusion (eg, intervertebral disc space, vertebral body, and pedicles).

Results: Electrical stimulation with electroactive pedicle screws at various stimulation amplitudes and anodization patterns enabled modulation of spatial distribution and intensity of electric fields within the target regions of lumbar spine. Anodized screws (50%) vs unanodized screws (0%) induced high-amplitude electric fields within the intervertebral disc space and vertebral body but negligible electric fields in spinal canal. Direct current electrical stimulation via anodized screws induced electrical fields, at therapeutic threshold of >1 mV/cm, sufficient for osteoinduction within the target interbody region.

Conclusions: Selective anodization of electroactive pedicle screws may enable focal delivery of therapeutic electrical stimulation in the target regions in human lumbar spine. This study warrants preclinical and clinical testing of integrated electroactive system in inducing target lumbar fusion in vivo.

Clinical Relevance: The findings of this study provide a foundation for clinically investigating electroactive intrumentation to enhance spine fusion.

Level of Evidence: 5.

New Technology

Keywords: interbody fusion, electrical stimulation, bioelectric therapy, osteogenesis, pseudarthrosis

INTRODUCTION

More than 400,000 spinal fusion procedures are performed every year in the United States.[1] As the older population has increased, the utilization of spinal fusion for degenerative etiology has also significantly increased over the past decade.[1] Despite advancements in surgical techniques, approximately 10% to 40% of spine fusions fail, leading to failed back surgery ultimately requiring revision surgeries.[2] There remains a classically defined "difficult to fuse" patient population, that is, elderly patients (>65 years old), osteoporotic patients undergoing multilevel fusion, and patients with multiple prior fusion surgeries.[3–5] Successful solid spinal fusion represents a significant clinical challenge for spine surgeons, and alternative therapies are needed to reliably augment fusion.

Electrical stimulation is a promising nonpharmacological adjunct enhancing bone growth following spine fusion.[6] Electrical stimulation modulates the physiological bioelectric state at the site of fusion, promoting osteoinduction of proliferating bone cells, thereby accelerating bone deposition and remodeling.[7,8] Various methods of electrical stimulation exist, including noninvasive pulsed electromagnetic fields and invasive direct current electrical stimulation.[9] Although useful, these systems do not create local electrical fields at the site of fusion, which is recognized as the most important factor increasing the efficacy of electrical stimulation therapy.[10,11]

To overcome these limitations, we developed an integrated electroactive implant system capable of combining strengths of rigid spinal instrumentation and
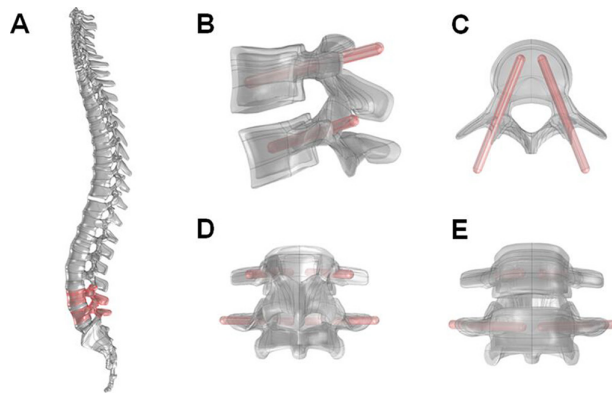
Figure 1. (A) Model of human lumbar spine with L4-L5 instrumentation. Four electroactive simplified pedicle screws instrumented at L4-L5 level simulated the clinical instrumentation and stabilization with (B) sagittal, (C) axial, (D) posterior, and (E) anterior views.
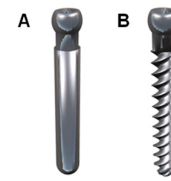

Figure 2. Model pedicle screws: (A) simplified and (B) threaded.

osteogenic potential of direct current electrical stimulation.[11] By modifying standard spinal rods and pedicle screws, cathodic direct current was routed through the spinal rods energizing implanted pedicle screws. This allowed focal delivery of electrical fields around the pedicles and vertebral bodies through conductive portions of the threaded pedicle screws (cathodes). Integrated osteogenic electroactive instrumentation may offer a unique alternative to existing spinal instrumentation. The primary aim of this study was to establish optimal parameters and evaluate the feasibility of electroactive instrumentation in focal delivery of therapeutic electrical stimulation to the target sites of fusion within the lumbar spine.

METHODS

Simulation of Single-Level Instrumentation With Electroactive Pedicle Screws

A normal adult human lumbar spine model with single-level fusion instrumentation with 4 pedicle screws at L4-L5 was simulated in COMSOL Multiphysics software V4.3 (COMSOL, Inc., Burlington, MA) (Figure 1). The vertebral model was placed in a homogenous, isotropic tissue volume (length = 0 cm, width = 10 cm, height = 10 cm) modeled as an independent subdomain having bulk material properties of saline (σ = 2.0 S/m). L4 and L5 vertebrae were isolated and manually subdivided into subdomains with bulk material properties consistent with cortical (σ = 4.52 mS/m transverse, σ = 64.52 mS/m horizontal) and trabecular bone (σ = 0.1642 S/m transverse, σ = 0.2 S/m horizontal).

Pedicle screws were modeled in COMSOL as a single, uniform subdomain having bulk material

properties consistent with medical grade titanium alloy (Ti6Al4V) (σ = 2.38 MS/m) with screw diameter of 6.0 mm and screw length of 40 mm. To determine the effect of surface topology of pedicle screws on induced electrical field distributions, pedicle screws were modeled in 2 patterns: (1) threaded: simulating clinical pedicle screws and (2) simplified: as round cylindrical rods (Figure 2). Pedicle screws were surface anodized with a layer of resistive titanium oxide (σ = 10 pS/m, thickness = 0–400 nm) located at the boundary of the metallic screw subdomain. To control the site of focal electrical stimulation, a uniform pattern with equal anodization thickness (ie, impedance) over screw length was varied between 0%, 50%, 75%, 90%, and 95% with only unanodized region representing conductive portion delivering electrical stimulation. Furthermore, a graded pattern of anodization was evaluated with anodization thickness graded over the entire (100%) length of screw or distal half (50%) in linear and exponential gradients.

Evaluation of Electrical Field Distribution Evoked by Electroactive Pedicle Screws

Electrical activation of model pedicle screws was simulated with current density (Neumann) boundary conditions of direct current stimulation amplitudes at 20, 40, 60, 80, and 100 μA. Boundary surfaces of the surrounding tissue volume were set as ground. The electroactive pedicle screw and surrounding tissue volume were discretized into ~1,000,000 tetrahedrons.

Electrical field distributions within the vertebrae and the surrounding tissue volume following activation of electroactive pedicle screws were calculated and plotted in singular colorimetric cross sections taken at multiple axes through the vertebral model. The amplitudes within the stimulated electric field were quantified as a function of orthogonal distance from midpoint of pedicle screws. The amplitude of >1 mV/cm was defined as threshold for osteogenic electric field. The distribution of electrical fields was evaluated for various configurations: (1) screw design (threaded vs simplified models), (2) varying stimulation amplitudes (20–100

μA), (3) patterns of anodization (uniform vs graded), and (4) length of the anodized region over the screw (0%–95%).

Evaluation of Focal Delivery of Electrical Stimulation to the Target Sites of Lumbar Fusion

Three target regions of interest (ROIs) for lumbar fusion were defined as the intervertebral disc space (L4-L5 interbody), vertebral body, and pedicles. Each region was defined as a set of multiplanar 2-dimensional surfaces consistent with anatomical dimensions. Osteogenic electrical stimuli were quantified within the target ROIs to evaluate the optimal configuration of electroactive pedicle screws. Electrical field distributions within the target ROIs were plotted in colorimetric sections in the axial plane through the center of L4-L5 intervertebral space and in the sagittal plane through the midline of the intervertebral space. Numerical data from nodes within defined ROIs were summed to determine mean values of induced electric fields within the anatomical region. Mean electric field amplitudes were calculated and plotted for various configurations of electroactive pedicle screw, including uniform vs graded patterns of anodization and variable length of anodized region.

RESULTS

Electrical Field Distributions at Various Electroactive Pedicle Screw Configurations

Screw Topology

Direct current electrical stimulation at 40 μA yielded the highest amplitude in an elliptical region surrounding the entire length of each screw (Figure 3). Electric
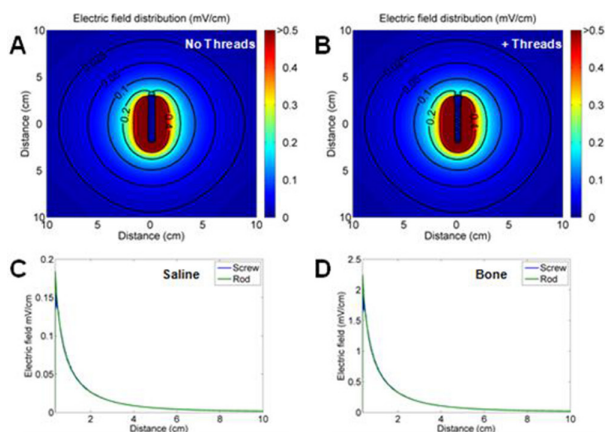

Figure 3. Electrical field distribution of electroactive pedicle screws implanted in the trabecular bone: (A) simplified screw and (B) threaded screw. Osteogenic electrical amplitude is concentrated in the elliptical region surrounding screws. The amplitude rapidly declined with increasing orthogonal distance from midpoint of each screw (C) in saline and (D) in trabecular bone.

fields induced by electroactive pedicle screws in saline (E_{max} = 0.18 mV/cm) were observed to be lower in intensity as compared with those induced in trabecular bone (E_{max} = 2.3 mV/cm). Electric field amplitudes rapidly declined with increasing distance from the midpoint of the pedicle screws. There were no significant differences between electric field distributions generated by simplified vs threaded pedicle screws at all positions except at the screw surface (Figure 3A and B, respectively). On high magnification (data not shown), simplified screws yielded uniform electrical field distribution along the smooth screw surface. In contrast, threaded screw resulted in focal regions of high-intensity electric fields at the crests of threaded screw surface.

Stimulation Amplitude

Increasing electrical stimulation amplitudes from 20 to 100 μA resulted in increased electrical field amplitudes and broader spatial region of osteogenic electric fields (>1 mV/cm) generated in trabecular bone surrounding the pedicle screws (Figure 4). All induced electrical fields had an elliptical pattern extending over the entire length of the screw. Stimulation of pedicle screws at 20 μA induced osteogenic electric field at only screw surface, while stimulation at 100 μA induced osteogenic electric field approximately 2 cm surrounding the screw surface (Figure 4A–E). Quantitative analysis revealed that increasing stimulus amplitude (current [I] = 20–100 μA) resulted in a progressive increase in the maximal electric field amplitude (E_{max} = 1.0–5.6 mV/cm) surrounding the electroactive pedicle screws (Figure 4F).
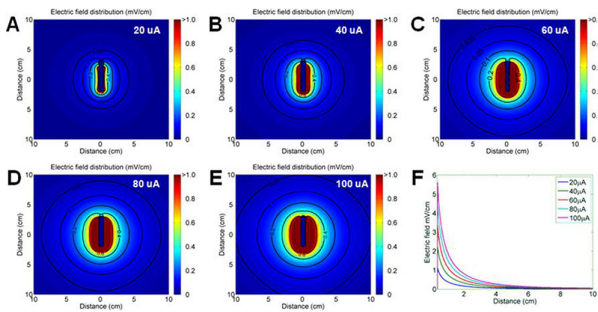
Anodization Patterns

Direct current electrical stimulation at constant amplitude of 40 μA revealed that surface anodization region significantly altered the geometry of induced electric fields (Figure 5). Unanodized pedicle screw (0% anodized) induced an elliptical electric field distribution extending along the entire length of the screw (Figure 5A), while anodized pedicle screws (50% anodized) induced a spherical electrical field distribution centered on the conductive portion (unanodized region) of the screw (Figure 5B). Progressive anodization of the pedicle screw body further concentrated the induced electrical field around the conductive screw tip (Figure 5C and D), thereby shifting the spatial region of osteogenic electric fields toward the distal tip of the screw. Anodization of >50% of the pedicle screw body (50%–95%) did not alter the spherical electric field geometry.
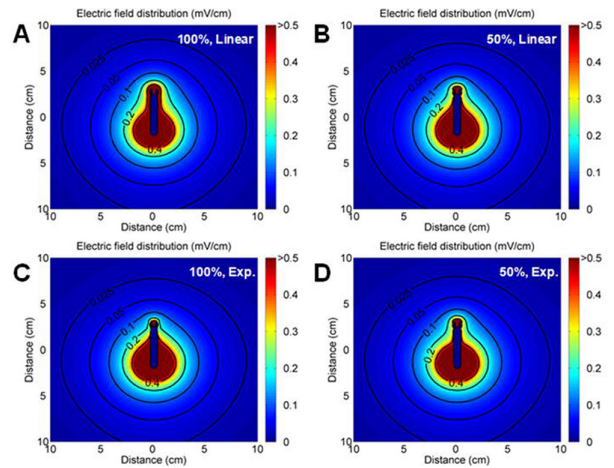
Figure 4. Electrical fields generated via electroactive simplified pedicle screws in trabecular bone. Osteogenic electrical field (>1 mv/cm) is represented as dark red on colorimetric scale surrounding the screw. (A–E) Electrical fields created by stimulation from 20 to 100 μA amplitudes. (F) Larger stimulus amplitude increased electrical field amplitude and distance orthogonal to midpoint of screw.

Spatial variance of anodization thickness (graded pattern) along the length of pedicle screws altered the geometry and amplitude of induced electric fields (Figure 6). Pedicle screws with linear gradient of anodization along the entire length (100%, linear) exhibited a "pear-shaped" electric field distribution with high-intensity osteogenic electrical fields focused distal to the screw tip (Figure 6A). Limiting the graded region of anodization to the distal half of the screw (50%, linear) maintained the high-amplitude electric field distribution at the distal tip of the screw (Figure 6B). Results were similar when pedicle screws were anodized with exponential gradient over the entire length (100%, exponential) (Figure 6C) or the distal half of the screw (50%, exponential) (Figure 6D).
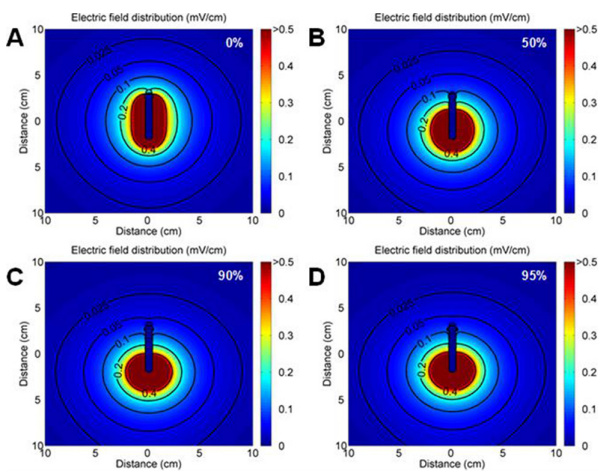
Figure 5. Effect of selective anodization with a uniform layer of 400 nm on electrical field distribution at constant stimulus amplitude of 40 μA around the pedicle screw. Osteogenic electrical field (>1 mv/cm) is represented as dark red on colorimetric scale surrounding the screw. (A) Without anodization. (B–D) Increasing anodization from 50% to 95% of the screw.


Figure 6. Effects of graded anodization of the screw body on electrical field distribution. (A) Gradient anodization (100% linear) and (B) gradient anodization limited to distal half of screw (50% linear). (C) Gradient anodization limited to distal half of screw (100% exponential). (D) Gradient anodization limited to distal half of screw (50% exponential). Osteogenic electrical field (>1 mv/cm) is represented as dark red on colorimetric scale surrounding the screw.

Focal Delivery of Osteogenic Electrical Stimuli to the Target Sites of Lumbar Fusion

At constant electrical stimulation amplitude of 40 μA, surface anodization patterns significantly changed both the anatomical distribution and amplitude of electric fields induced within the target ROIs (Figure 7). Unanodized pedicle screws (0% anodized) induced only low-amplitude electric fields within the intervertebral space and moderate electrical fields within the cortical bone of instrumented pedicles. In contrast, anodized pedicle screws (50% anodized) induced high-amplitude electric fields within the intervertebral space and moderate electrical fields within the instrumented pedicles. Increasing anodization of longer portions of the pedicle screw shifted the spatial region of osteogenic electrical fields within the anterior and posterior regions of the intervertebral space and anterior trabecular and cortical regions of the L4 vertebral body. However, it decreased the amplitude of similar fields within the instrumented pedicles (Figure 7).

At a constant electrical stimulation amplitude of 40 μA, graded anodization patterns induced higher amplitude electric fields within the intervertebral space, L4 vertebra, and instrumented pedicles than unanodized pedicle screws (0% anodized) (Figure 7). Graded anodization with linear gradients demonstrated higher amplitude electric fields within the pedicles compared with matched screws anodized with exponential gradients (Figure 7).
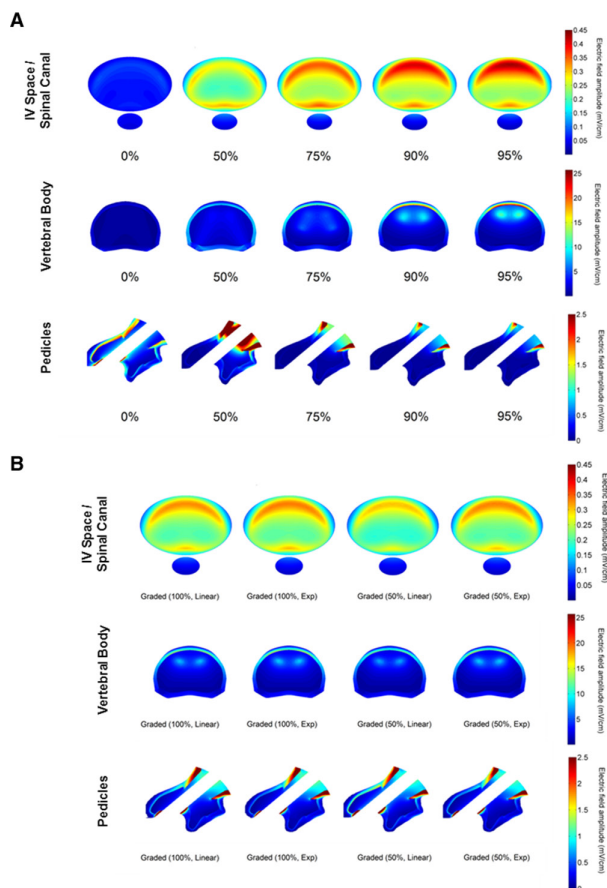
Figure 7. The osteogenic electrical field distribution in regions of interest of L4-L5 level (A) by varying percentage of anodization and (B) gradient vs exponential anodization of electroactive pedicle screws at constant electrical stimulation amplitude of 40 µA. Increasing anodization to 50% focused osteogenic electrical field within the intervertebral (IV) space, vertebra, and instrumented pedicles. Screw anodization of >50% further focused osteogenic electrical field in the intervertebral space, anterior vertebral body, however, reduced in the instrumented pedicles. Similarly, increasing gradient anodization (both linear and exponential) resulted in osteogenic electric fields within the intervertebral space, vertebra, and instrumented pedicles.

DISCUSSION

We developed a novel system that integrates promising nonpharmacologic electrical stimulation with existing instrumentation into a unique electroactive system capable of providing both mechanical stabilization and targeted osteogenic stimulation of the spine.[11] In this biocomputational study, we established the optimal parameters for osteogenic electrical stimulation using this unique electroactive system for induction of bone regeneration in the normal spine. Our findings suggest that manipulation of electroactive pedicle screws in various combinations of anodization patterns and stimulus amplitudes has the potential to provide bone stimulation in the target areas of lumbar spine individualized to various fusion procedures.

Electrical stimulation has been suggested as a promising nonpharmacological adjunct to enhance bony regeneration and fusion. It has been demonstrated that normal bone exhibits pronounced electronegativity, and following injury, the electrical potential serves as a cellular cue promoting bone cell migration, proliferation, and differentiation.[8,12,13] Direct current electrical stimulation has been demonstrated to accelerate bone formation and healing in the lumbar spine.[14–19] Recent developments in spine surgery guidelines suggest the use of electrical stimulators for high-risk patient population.[20]

Despite these advances, utilization of direct current electrical stimulation has not gained widespread adoption in spinal fusion procedures. Existing electrical stimulators are limited by bulky implantable hardware, incompatibility with rigid instrumentation, and an inability to induce interbody fusion.[20,21] This highlights the significant need of improvement in existing electrical stimulator technology to enhance the spine fusion. An integrated system combining the strength of existing implant/graft technologies and nonpharmacological electrical stimulation may substantially enhance rates of solid spinal fusion.[11] The primary aim of this study was to evaluate the capability of this unique system in the delivery of targeted electrical stimulation to the target sites of spine fusion.

In the uniform tissue model, we found that unanodized (0%) electroactive pedicle screws created only diffuse low-amplitude electrical fields modulated by various stimulus amplitudes and remained below the osteogenic thresholds. In contrast, selective anodization of pedicle screws enabled a wide range of induced osteogenic electrical fields and amplitudes modulated by anodization parameters including length, thickness, and gradient of anodization.

In the in vivo human lumbar spine model, electrical stimulation by unanodized pedicle screws (0% anodized) failed to induce osteogenic electrical fields within the intervertebral space and vertebral body. In contrast, electrical stimulation by anodization of pedicle screws (50% anodized) induced high-amplitude osteogenic electrical fields in the target regions of fusion in lumbar spine (ie, intervertebral space, vertebral body, and cortical bone around the electroactive pedicle screws). These findings suggest the controllable and tunable nature of this osteoinductive system such that by selective anodization of pedicle screws the delivery of therapeutic electric fields may be focused on target sites of fusion without inducing concomitant fusion in unwanted regions (ie, spinal canal).

The optimal stimulation amplitude associated with increased bone density in lumbar fusion remains

unknown. Multiple studies have examined the role of direct current electrical stimulation on the bone formation in both in vitro, in vivo preclinical, and human clinical settings.[6,9,22] Generally, low-current amplitudes do not provide enough stimulation while high-current amplitudes may induce osteonecrosis of nascent bone cells at the site of fusion.[22] Perhaps an ideal current amplitude depends upon multiple factors including density of underlying bone, surface area, and length of stimulation. While no single optimal stimulation amplitude has been demonstrated, the literature concludes that the optimal range of stimulation amplitudes exists between 20 and 100 uA.[9] Specifically, commercially available devices utilizing direct current electrical stimulation to promote bone formation and bony fusion utilize 40 and 60 uA, respectively (eg, SpF system).[23] Further work is needed to identify the optimal stimulation parameters needed to optimize bone formation and fusion in the setting of lumbar interbody fusion.

Considering the close vicinity of electroactive pedicle screws with the neurological tissue, there remains a concern of neurological injury or inadvertent modulation. However, the risk to neurological injury using this osteogenic system is minimal as the amplitude of stimulation is capped at a reasonable level. Neural tissue particularly responds to higher frequencies of electrical stimulation (10–60+ Hz) and does not respond to direct current electrical stimulation. Therefore, the risk of neural excitation or aberrant modulation is minimal. As long the electroactive screws are placed within the pedicle and the stimulation amplitude is modulated in a safe range, the risk of neurological injury is minimal, on par with other deep brain stimulation or pacemaker style devices.

In a prior in vivo study, our group utilized a goat interbody fusion model to test the effect of electroactive spine instrumentation.[11] We utilized a microscale implantable power generator (similar to a pacemaker) to provide power and communication to the electroactive osteogenic pedicle screws. This implantable power generator was connected via a flexible microwire to the screws such that instrumentation was not affected or complicated. While human testing is warranted, our study demonstrated that integrated osteogenic system led to focal enhancement in the lumbar interbody fusion.[11] In addition, in vivo studies in sheep and goat lumbar interbody fusion models showed stable electrical stimulation over multiple months with minimal complications.[24] An alternative to implantable power generator is the wireless power transduction as a means of powering the electroactive pedicle screws.
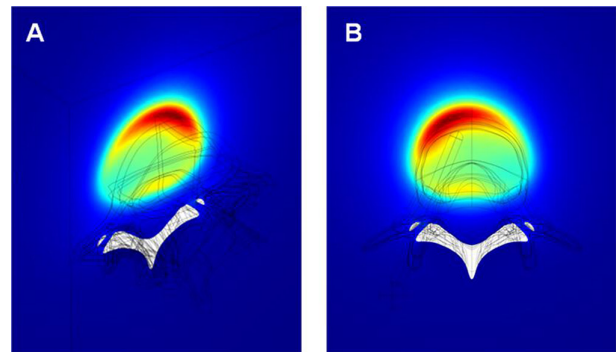
Figure 8. A 3-dimensional spinal model of L4-L5 intervertebral space with colorimetric plot of osteogenic electrical field distribution: (A) oblique and (B) axial views after stimulation of 1 instrumented electroactive pedicle screw.

Our results demonstrate the capability of selective anodization in stimulating various anatomical and spatial locales around the spine. For example, a linear anodization pattern focused the dense osteogenic electrical field inducing bone formation in proximity to the screw tip at the anterior third of the intervertebral space. This region might reinforce the fusion mass formation in the anterior column promoting lumbar interbody fusion, preventing graft subsidence, and maintaining achieved indirect decompression/lordosis.[25,26] Additionally, selective anodization with a gradient linear pattern focused on the osteogenic electrical fields within the pedicles may strengthen the screw purchase, potentially preventing implant loosening and pull out.[27,28] Directional/spatial guidance of the direct current electrical stimulation is expected to translate to a safer and more effective therapy. A cross-section of L4-L5 vertebrae instrumented with electroactive pedicle screw and resulting electric field distribution in 2-dimensional colorimetric plot across intervertebral space is shown in Figure 8.

Limitations

This study has several limitations. First, we included a limited number of anatomical structures, which do not fully reflect the anatomical landscape of the lumbar spine. Second, we assessed only key ROIs, therefore overall percent of bone volume reaching the threshold for osteogenic stimuli may be underestimated. Clinical implementation of spinal hardware may utilize a variable number of pedicle screws. Therefore, in vivo electric field amplitudes may largely be assumed to be a sum of electric field distributions, variably overlaid, and centered around the fusion site. Finally, since this study aimed to demonstrate feasibility, our model assumed that electroactive pedicle screws were implanted in a normal spine. Therefore, these results

are only applicable to young healthy adults without any spine pathology. In future studies, the utility of electroactive pedicle screws modeled with various anodization patterns tailored to the specific pathology, level, or depth of instrumentation should be explored. Despite these limitations, this system may provide tailored electrostimulation protocols individualized to specific spine fusion procedures.

CONCLUSIONS

This study provides a proof of concept of electroactive spinal instrumentation in focal delivery of therapeutic electrical stimulation to target sites of lumbar spinal fusion. Selective anodization of pedicle screws may enable osteogenesis in select anatomical locations at the target fusion site. Furthermore, the manipulation of anodization patterns of electroactive pedicle screws can focus electrical stimulation at specific anatomical regions. Our results suggest that 95% anodization of pedicle screw body with a constant 400 nm layer of titanium oxide may induce high-intensity electric fields within the intervertebral disc space and vertebral body without osteogenic stimulation of the spinal canal. This study warrants further investigation of an integrated system of electroactive instrumentation in delivery of therapeutic electrical stimulation in vivo.

REFERENCES

1. Rajaee SS, Bae HW, Kanim LEA, Delamarter RB. Spinal fusion in the United States: analysis of trends from 1998 to 2008. *Spine (Phila Pa 1976)*. 2012;37(1):67–76. doi:10.1097/BRS.0b013e31820cccfb

2. Adogwa O, Carr RK, Kudyba K, et al. Revision lumbar surgery in elderly patients with symptomatic pseudarthrosis, adjacent-segment disease, or same-level recurrent stenosis. Part 1. two-year outcomes and clinical efficacy: clinical article. *J Neurosurg Spine*. 2013;18(2):139–146. doi:10.3171/2012.11.SPINE12224

3. Kim YJ, Bridwell KH, Lenke LG, Rhim S, Cheh G. Pseudarthrosis in long adult spinal deformity instrumentation and fusion to the sacrum: prevalence and risk factor analysis of 144 cases. *Spine (Phila Pa 1976)*. 2006;31(20):2329–2336. doi:10.1097/01.brs.0000238968.82799.d9

4. Bydon M, De la Garza-Ramos R, Abt NB, et al. Impact of smoking on complication and pseudarthrosis rates after single- and 2-level posterolateral fusion of the lumbar spine. *Spine (Phila Pa 1976)*. 2014;39(21):1765–1770. doi:10.1097/BRS.0000000000000527

5. Adogwa O, Parker SL, Shau D, et al. Long-Term outcomes of revision fusion for lumbar pseudarthrosis: clinical article. *J Neurosurg Spine*. 2011;15(4):393–398. doi:10.3171/2011.4.SPINE10822

6. Cottrill E, Pennington Z, Ahmed AK, et al. The effect of electrical stimulation therapies on spinal fusion: a cross-disciplinary systematic review and meta-analysis of the preclinical and clinical data. *J Neurosurg Spine*. 2019:1–21. doi:10.3171/2019.5.SPINE19465

7. Leppik L, Zhihua H, Mobini S, et al. Combining electrical stimulation and tissue engineering to treat large bone defects in a rat model. *Sci Rep*. 2018;8(1):6307. doi:10.1038/s41598-018-24892-0

8. Eischen-Loges M, Oliveira KMC, Bhavsar MB, Barker JH, Leppik L. Pretreating mesenchymal stem cells with electrical stimulation causes sustained long-lasting pro-osteogenic effects. *PeerJ*. 2018;6:e4959. doi:10.7717/peerj.4959

9. Khalifeh JM, Zohny Z, MacEwan M, et al. Electrical stimulation and bone healing: a review of current technology and clinical applications. *IEEE Rev Biomed Eng*. 2018;11:217–232. doi:10.1109/RBME.2018.2799189

10. Yao G, Kang L, Li C, et al. A self-powered implantable and bioresorbable electrostimulation device for biofeedback bone fracture healing. *Proc Natl Acad Sci U S A*. 2021;118(28):e2100772118. doi:10.1073/pnas.2100772118

11. MacEwan MR, Talcott MR, Moran DW, Leuthardt EC. Novel spinal instrumentation to enhance osteogenesis and fusion: a preliminary study. *J Neurosurg Spine*. 2016;25(3):318–327. doi:10.3171/2016.1.SPINE13979

12. Yuan X, Arkonac DE, Chao PG, Vunjak-Novakovic G. Electrical stimulation enhances cell migration and integrative repair in the meniscus. *Sci Rep*. 2014;4:3674. doi:10.1038/srep03674

13. Ercan B, Webster TJ. Greater osteoblast proliferation on anodized nanotubular titanium upon electrical stimulation. *Int J Nanomedicine*. 2008;3(4):477–485. doi:10.2147/ijn.s3780

14. Dwyer AF, Wickham GG. Direct current stimulation in spinal fusion. *Med J Aust*. 1974;1(3):73–75. doi:10.5694/j.1326-5377.1974.tb50762.x

15. Kane WJ. Direct current electrical bone growth stimulation for spinal fusion. *Spine*. 1988;13(3):363–365. doi:10.1097/00007632-198803000-00026

16. Meril AJ. Direct current stimulation of allograft in anterior and posterior lumbar interbody fusions. *Spine*. 1994;19(21):2393–2398. doi:10.1097/00007632-199411000-00004

17. Rogozinski A, Rogozinski C. Efficacy of implanted bone growth stimulation in instrumented lumbosacral spinal fusion. *Spine (Phila Pa 1976)*. 1996;21(21):2479–2483. doi:10.1097/00007632-199611010-00014

18. Kucharzyk DW. A controlled prospective outcome study of implantable electrical stimulation with spinal instrumentation in A high-risk spinal fusion population. *Spine (Phila Pa 1976)*. 1999;24(5):465–468. doi:10.1097/00007632-199903010-00012

19. Tejano NA, Puno R, Ignacio JM. The use of implantable direct current stimulation in multilevel spinal fusion without instrumentation. A prospective clinical and radiographic evaluation with long-term follow-up. *Spine (Phila Pa 1976)*. 1996;21(16):1904–1908. doi:10.1097/00007632-199608150-00015

20. Kaiser MG, Eck JC, Groff MW, et al. Guideline update for the performance of fusion procedures for degenerative disease of the lumbar spine. Part 17: bone growth stimulators as an adjunct for lumbar fusion. *J Neurosurg Spine*. 2014;21(1):133–139. doi:10.3171/2014.4.SPINE14326

21. Bhavsar MB, Han Z, DeCoster T, Leppik L, Costa Oliveira KM, Barker JH. Electrical stimulation-based bone fracture treatment, if it works so well why do not more surgeons use it? *Eur J Trauma Emerg Surg*. 2020;46(2):245–264. doi:10.1007/s00068-019-01127-z

22. Black J, Baranowski TJ, Brighton CT. Electrochemical aspects of D.C. stimulation of osteogenesis. *Bioelectrochemistry and Bioenergetics*. 1984;12(3–4):323–327. doi:10.1016/0302-4598(84)87012-9

23. Jenis LG, An HS, Stein R, Young B. Prospective comparison of the effect of direct current electrical stimulation and pulsed electromagnetic fields on instrumented posterolateral lumbar arthrodesis. *J Spinal Disord*. 2000;13(4):290–296. doi:10.1097/00002517-200008000-00004

24. Toth JM, Seim HB 3rd, Schwardt JD, Humphrey WB, Wallskog JA, Turner AS. Direct current electrical stimulation increases the fusion rate of spinal fusion cages. *Spine (Phila Pa 1976)*. 2000;25(20):2580–2587. doi:10.1097/00007632-200010150-00007

25. Shen H, Chen Y, Liao Z, Liu W. Biomechanical evaluation of anterior lumbar interbody fusion with various fixation options: finite element analysis of static and vibration conditions. *Clin Biomech (Bristol, Avon)*. 2021;84:105339. doi:10.1016/j.clinbiomech.2021.105339

26. Ding Q, Tang X, Zhang R, Wu H, Liu C. Do radiographic results of transforaminal lumbar interbody fusion vary with cage position in patients with degenerative lumbar diseases? *Orthop Surg*. 2022;14(4):730–741. doi:10.1111/os.13224

27. Marie-Hardy L, Pascal-Moussellard H, Barnaba A, Bonaccorsi R, Scemama C. Screw loosening in posterior spine fusion: prevalence and risk factors. *Global Spine J*. 2020;10(5):598–602. doi:10.1177/2192568219864341

28. Burval DJ, McLain RF, Milks R, Inceoglu S. Primary pedicle screw augmentation in osteoporotic lumbar vertebrae: biomechanical analysis of pedicle fixation strength. *Spine (Phila Pa 1976)*. 2007;32(10):1077–1083. doi:10.1097/01.brs.0000261566.38422.40

Corresponding Author: Matthew R. MacEwan, Department of Neurosurgery, Washington University School of Medicine, 660 S Euclid Ave, Campus Box 8057, St. Louis, MO 63110, USA; macewanm@wustl.edu